Reactor modelling for rf plasma deposition of Si_xN_y-H. Comparison between two flow arrangements.

H.Caquineau, G.Dupont and B. Despax

Laboratoire de Génie Electrique, URA 304 du CNRS, Université Paul Sabatier, 118 route de Narbonne, 31062 Toulouse Cédex, France

Abstract: Plasma deposition processes involve complex phenomena which make the design and optimization of industrial equipments difficult. In the particular case of silane-ammonia plasmas to produce silicon nitride (at very low silane percentage), two flow arrangements were studied by numerical modelling of mass transport. The modelling of a long parallel plate reactor shows a decrease of silane concentration from inlet to outlet and a steep decrease of deposition rate along the flow direction. A radial flow reactor with a distributed gas feed by means of a "showerhead" electrode,achieves a more uniform deposition rate under all experimental conditions.

INTRODUCTION

Plasma-assisted deposition of silicon-nitride thin films, using a radiofrequency (rf) glow discharge of SiH_4-NH_3 mixtures, is widely used in microelectronics. Although research in the field produced a significant collection of data, the industrial use of acquired knowledge poses several problems. In large industrial PECVD machines, the choice of the gas flow arrangement plays a particularly important role. However, this subject has seldom been treated in the literature, because its experimental approach would involve important investments to build the needed equipment. Recently, numerical modelling for SiN-H deposition in a long parallel plate reactor has been developed [1,2]. This paper suggests how a theoretical treatment, using modelling and numerical simulation, can help in that field. Numerical simulations will compare two different geometries and gas flow organizations and the effects on the deposition profile.

I- TWO DIMENSIONAL MODELS

The first model of the long parallel plate reactor used throughout this work has already been presented in details elsewhere [1,2]. The second modelling of flow organization involves a radial flow reactor with a "showerhead" electrode. They were developed to deal with the particular case of silicon nitride deposition from silane-ammonia mixtures, in the rf plasma reactors schematically described in Figure 1.

Such a model treats three important groups of phenomena, the electron-molecule interactions which determine the electrical characteristics of the plasma, then the transports in the gas phase which involve the homogeneous chemistry of the active species produced by electron impacts with the other molecules, and the surface reactions which lead to the deposit.

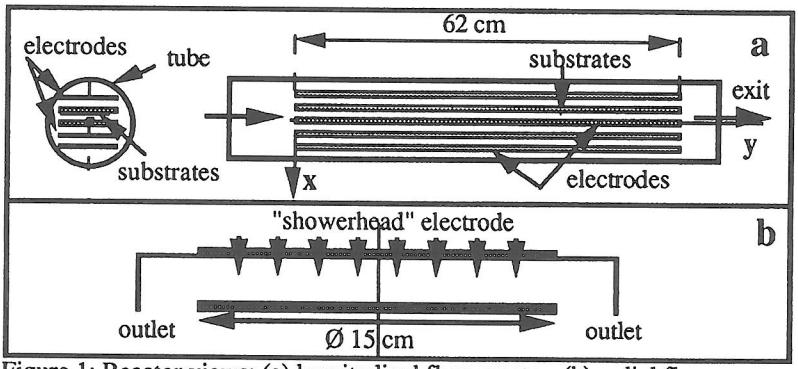

Figure 1: Reactor views: (a) longitudinal flow reactor, (b) radial flow reactor

I.1. Electron-molecule interactions

The complete electrical characteristics of the plasma have been estimated by using an rf discharge fluid model, recently developed by JP. Boeuf and Ph. Belenguer [3], that allows the determination of dissociation, attachment and ionization rate profiles in the interelectrode space.The dissociation rate profiles averaged over one rf cycle present two local maxima in the immediate vicinity of the electrodes, corresponding to the regions where electrons release a maximum of energy when colliding with molecules, and an approximately flat region in the center (positive column). More information on the modelling of rf discharges can be found in reference 4.

Due to the very low silane concentration considered here, the main dissociation products are NH2, NH and H, while the contribution of electron impact to silane radical production remains low.

I.2. Chemistry and reactive transport

a) Chemistry

The experimental data were previously discussed in detail elsewhere [1,2]. To sum up, the literature survey highlights that silicon nitride deposition chemistry is complex and leads mostly to disilane and aminosilane formation [5,6]. Moreover, these data also show that the aminosilane formation follows different steps involving the aminosilane radical intermediates.The gas phase chemistry considered here brings into play, first an initial step of silane radical formation due to the hydrogen abstraction on silane, then a reasonable mechanism of radical-radical reaction forming a vibrationnally activated complex, which leads to either radical propagation or stable species formation. Indeed, the collisional stabilization of the nascent, vibrationnally excited product favors stable species formation to the detriment of radical propagation, depending on pressure conditions. Finally, hydrogen abstraction on aminosilane coupled with a very low reactivity of NH_2 with the $Si(NH_2)_3$ radical is necessary to explain the amazingly high level of the triaminosilane radical concentration experimentally observed by Smith and Jasinski [5,6]. The homogeneous chemical mechanism that was selected is presented in Figure2: the corresponding kinetic constants (not presented here, ref 1,2,4.) were taken from the literature and eventually corrected using a QRRK method [7] to adjust to the operating conditions used in this work.

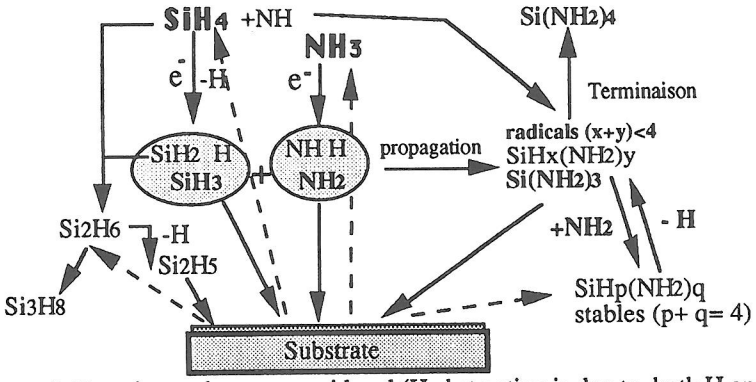

Figure 2: Reaction pathways considered (H abstraction is due to both H and NH2 radicals respectively producing the secondary products H2 and NH3)

b) Mass transport

The analyses of gas flow and species transport were treated separately. Such an important simplification can only be used when the gaseous composition variations from the entrance to the exit of the reactor remain weak, so that the volume rate of flow and gas physical properties (density, viscosity...) may be considered as constants.

The partial differential equations of conservation of momentum and mass for each species were successively solved, in steady state and at constant temperature.

I.3. Surface reactions

The active species, created in the gas phase, that were taken into account on the surface are: SiH_3, SiH_2, Si_2H_5, NH_2, H, $HSiNH_2$, $Si(NH_2)_2$, $HSi(NH_2)_2$, $Si(NH_2)_3$ (Table I)

species	β	s	γ	bulk	recombination products
SiH_3, Si_2H_5	0.2	0.1	0.1	s (Si)	$(3/2)sH_2 + \gamma SiH_4 - (1/2)\gamma H_2$ $(3/2)sH_2 + \gamma Si_2H_6 - (1/2)\gamma H_2$
SiH_2	1	1	0	s (Si)	sH_2
NH_2	0 - 0.05	0 - 0.005	0	s (N)	sH_2
NH	0	0	0	-	-
H	0-1	0	0-1	-	$(1/2)\beta H_2$
$HSiNH_2$	0.01	0.01	0	s (Si-N)	$(3/2)sH_2$
$Si(NH_2)_2$	0.01	0.01	0	s (N-Si-N)	$2sH_2$
H_2SiNH_2	0.011	0.003	0.008	s (Si-N)	$2sH_2 + \gamma H_3SiNH_2$ $- (1/2)\gamma H_2$
$HSi(NH_2)_2$	0.0085	0.0025	0.006	s (N-Si-N)	$(5/2)sH_2 + \gamma H_2Si(NH_2)_2$ $- (1/2)\gamma H_2$
$Si(NH_2)_3$	0.006	0.002	0.004	s (N-Si-N)	$2sH_2 + sNH_3 + \gamma HSi(NH_2)_3$ $- (1/2)\gamma H_2 - (1/2)sH_2$

Table I: surface mechanism and selected reaction probabilities ($\beta = s+\gamma$)

The reactivity of the aminosilane species was experimentally found to be low [5]. The reaction probability values are: $10^{-3} < \beta = s$ (sticking coefficient)$+ \gamma$ (recombination

coefficient) $\leq 1.1\ 10^{-2}$. The values used for SiH_3, SiH_2 and H are around those considered for a-Si:H deposition [8]. Undoubtedly, the values taken for this study remain questionable, but only new quantitative experimental measurements would provide reliable information. From the reaction probability values by using classical kinetic theory, a macroscopic balance is written for each species comming into the model through boundary conditions.

II - GAS FLOW ORGANIZATION INFLUENCE

The oblong parallel plate reactor is schematically represented in Figure 1a. The gas enters the plasma on one reactor side and flows along the interelectrode space to the opposite end.

The first organization is compared with the one presented in Figure 1b which involves a gas feed distributed by means of a "showerhead" electrode providing a homogeneous gas supply over the full surface of the electrode. Gases are pumped away through the annular outlet located around the grounded electrode, which produces a radially symmetrical flow.

The results obtained with these gas flow systems are now compared in detail.

II.1 Velocity profiles

With the first reactor, flow is mainly in the longitudinal direction and rapidly reaches a parabolic profile, in perfect agreement with the well-known solution for flow between two parallel planes in laminar regime. When using the second reactor, gas is introduced through the "showerhead" electrode with a constant axial velocity. Its movement quite immediately changes to a radial flow, with a velocity which increases from the symmetry axis to the exit.

II.2. Deposition rates

Figure 3a presents both the calculated deposition rate profile and the composition profile (N/Si ratio) for the longitudinal flow reactor. It should be noted that the deposition rate is in good agreement with the experimental rate, except near the exit region where a retrodiffusion flux of silane flowing outside the interelectrode space can feed the reactor end. This effect cannot be taken into account in the two-dimensional model because of geometrical simplifications. Let us also point out both the thickness and the composition inhomogeneity along the flow direction. The analysis of the modelling results allows us to explain these inhomogeneities. The thickness inhomogeneity is directly linked to the silane consumption, which is complete in the middle of the reactor. In fact, in a SiH_4-NH_3 discharge, two classes of active species are involved: the silane radicals and the aminosilane radicals. The former radicals appear only in the first step of silane conversion, whereas the latter radicals are due to successive reactions with first class radicals. The most representative species of each class are SiH3 and $Si(NH_2)_3$. Thus, in the first half of the reactor, when SiH_4 is still present, the main deposit precursor is SiH_3. Later, when SiH_4 conversion is total, the main deposit precursor becomes $Si(NH_2)_3$, which has a substantially lower sticking coefficient than SiH_3, leading to low deposition rates in the second half of the reactor. Of course, the evolution of the main deposit precursor from SiH_3 to $Si(NH_2)_3$ also explain the increase of the N/Si ratio from the inlet towards the outlet.

For the radial flow reactor, at very low flow rate, high rf power, and low silane concentration (Fig.3b), the silane molar fraction remains low in the whole reactor (≈ 0.1 %): its conversion to aminosilane is almost total. Hence, the N/Si ratio of the deposit is

high, since $Si(NH_2)_3$ is the main deposit precursor. Moreover, radial $Si(NH_2)_3$ concentration variations near the substrate are less than 25 %, leading to good thickness and composition uniformity. The decrease of the deposition rate near the exit is due to the disappearance of $Si(NH_2)_3$ on the lateral wall.

II.3. Evolution of plasma composition and deposition rate versus rf power and SiH4 flow rate

- Longitudinal flow reactor

Figure 4 shows the theoretical evolution of the deposition rate profile as a function of silane percentage and electrical power along the flow direction. Increasing the silane molar silane percentage or decreasing the power leads to a better uniformity of thickness but the composition of the deposited films shifts to silicon-over-rich. The silicon excess affects the dielectric properties of the deposited layers.

- Radial flow reactor

In Figure 5a, the triaminosilane radical concentration correlates well with the deposition rate, except for lower power where silyl radicals contribute to the deposition process. Let us mention that above 8W of power, silane is strongly consumed, the deposition rate saturates and the film has an excess of N. Figure 5b shows the dependence of several product contributions and of the deposition rate on the SiH_4 flow rate. Notice that at low flow rate the deposition rate rises in proportion to the $Si(NH_2)_3$ molar fraction . At higher silane flow, the $Si(NH_2)_3$ concentration falls off, the silyl molar fraction increases and the deposition rate rises less steeply.

CONCLUSION

The model prediction was very clearly demonstrated in case of a longitudinal flow by the agreement between the results and the corresponding experimental data. Furthermore, the work showed that a coherent chemistry, supported by experimental data, justifies using theory and calculations to predict the results which would be obtained with another reactor gas flow organization. The analysis of the modelling results showed that the relative importance of the different phenomena brought into play depends both on the reactor design and the experimental conditions.The interest of the radial flow arrangement is clearly demonstrated: the deposition rate is much more uniform as a result of a far better uniformity of the concentration of the species involved in the plasma process. It is anticipated that it would be much more interesting with a larger equipment and a higher deposition rate.

REFERENCES

[1] A. Dollet, JP. Couderc and B. Despax, Plasma Sources Sci. Technol. 4, 94(1995)
[2] A. Dollet, JP. Couderc and B. Despax, Plasma Sources Sci. Technol. 4, 107(1995)
[3] JP. Boeuf and P. Belenguer personal communication
[4] A.Dollet, Thesis Université Paul Sabatier (Toulouse- France) 1993
[5] D.L. Smith, S.A.Alimonda, C.C. Chen, S.E.Ready, and B. Wacker, J. Electrochem. Soc., 137, 2, 614 (1990)
[6] D.B. Beach and J.M.Jasinski, J. Phys. Chem., 94, 3019 (1990)
[7] F. Communal, P.R. Westmoreland, Chemical and Physical Processes in Combustion, 98, 1, (1990)
[8] A. Matsuda; K. Nomoto, Y; Yakeuchi, A. Suzuki, A. Yuuki, J. Perrin, Surface Science, 227, 50, (1990)

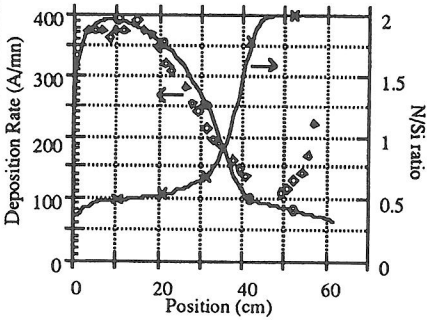

Fig. 3a: Theorical (o) and experimental (◊) deposition rate, and theorical N/Si ratio (x) vs. position in case a (reference conditions: P = 1 torr, T = 573 K, W = 100 W, Q = 1000 sccm, % SiH4 =4)

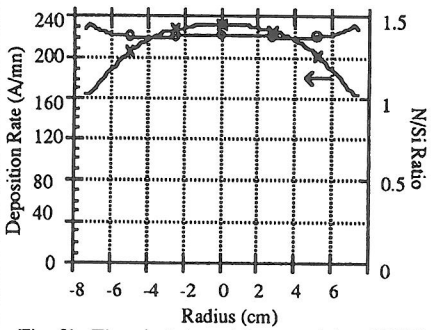

Fig. 3b: Theorical deposition rate (x) and N/Si ratio (o) vs. position in case b (reference conditions: P = 1 torr, T = 573 K, W = 11 W, Q = 47 sscm, % SiH4 = 4)

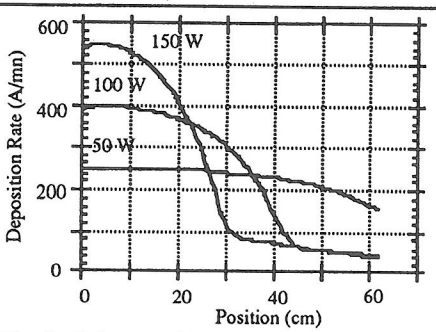

Fig. 4a: Influence of input power on deposition rate profile in case a (ref. conditions)

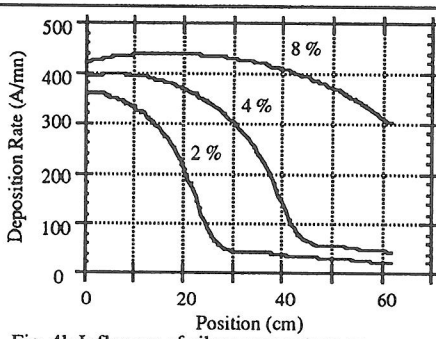

Fig. 4b:Influence of silane percentage on deposition rate profile in case a (ref. conditions)

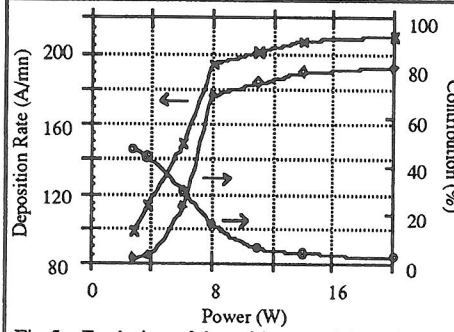

Fig 5a: Evolution of deposition rate (x) and contribution of SiH3 (o) and Si(NH2)3 (◊) with power in case b (ref. conditions)

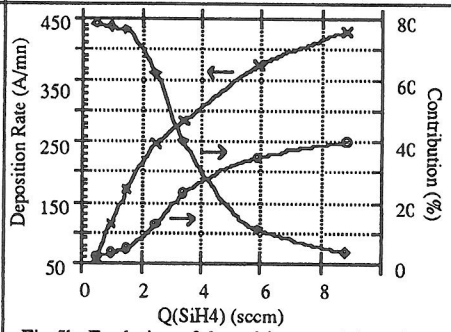

Fig 5b: Evolution of deposition rate (x) and contribution of SiH3 (o) and Si(NH2)3 (◊) with SiH4 flow rate in case b (ref. conditions)